International Journal for Multidisciplinary Research (IJFMR)
E-ISSN: 2582-2160 ● Website: www.ijfmr.com ● Email: editor@ijfmr.com

Comparative In-Silico Evaluation of Papain Like Protease (PLpro) Inhibitors Against SARS COV-2

Prerna Pradeep Bhosale[1], Yash Bhand[2], Hitesh Choudhary[3], Ajay Bichukale[4], Meeti Mahaur[5]

[1,2,3,4]Department of Pharmaceutical Chemistry, St. Wilfred Institute Of Pharmacy
[5]Assistant Professor,Department of Pharmaceutical Chemistry, St. Wilfred Institute Of Pharmacy

Abstract

Papain-Like Protease (PLpro) plays a critical role in viral polyprotein processing and suppression of the host immune response, making it an attractive target for antiviral drug discovery. The present study aimed to perform a comparative in silico evaluation of three reported PLpro inhibitors—GRL-0617, VIR-250, and VIR-251—against the crystal structure of SARS-CoV-2 PLpro (Protein Data Bank (PDB) ID: 7JRN). Molecular docking was carried out using UCSF (University of California, San Francisco) Chimera integrated with AutoDock Vina to evaluate binding affinity, ligand orientation, and protein–ligand interactions. The docked complexes were further analysed using BIOVIA Discovery Studio and Swiss ADME was employed to assess drug-likeness and pharmacokinetic properties. Among the selected inhibitors, GRL-0617 exhibited the highest binding affinity with a docking score of −7.7 kcal/mol, followed by VIR-251 (−7.5 kcal/mol) and VIR-250 (−7.2 kcal/mol). The favourable docking scores and low Root Mean Square Deviation (RMSD) values indicated stable binding conformations within the PLpro active site. Interaction analysis revealed the presence of key hydrogen bonds and hydrophobic interactions that contribute to ligand stability. Overall, the findings suggest that GRL-0617 is the most promising inhibitor among the compounds evaluated. This study demonstrates the usefulness of computational approaches in identifying potential antiviral candidates and provides a basis for further in-vitro and in-vivo investigations targeting SARS-CoV-2 PLpro.

Table.I. Dockscore Of Ligands

Ligands	Dockscore
GRL-0167	-7.7
VIR-250	-7.2
VIR-251	-7.5

Introduction

The COVID-19 pandemic emphasized the need for rapid development of effective antiviral therapies against SARS-CoV-2. This study focuses on the in-silico evaluation of selected Papain-Like Protease (PLpro) inhibitors to understand their binding interactions and identify promising drug candidates. The findings may contribute to future research aimed at developing effective treatments for COVID-19.

Coronavirus disease 2019 (COVID-19) is an infectious respiratory disease caused by the severe acute respiratory syndrome coronavirus 2 (SARS-CoV-2). First identified in late 2019, the virus rapidly spread across the globe, leading the World Health Organization (WHO) to declare COVID-19 a pandemic on 11 March 2020. The disease primarily spreads through respiratory droplets and close human contact. While most infected individuals experience mild to moderate symptoms, elderly people and those with underlying medical conditions are at a greater risk of developing severe illness and complications. WHO played a crucial role in coordinating international research efforts, monitoring disease transmission, and supporting the development of diagnostic tools, vaccines, and therapeutic agents to control the pandemic. [1–10]

SARS-CoV-2 enters human cells through interactions between its spike protein and host cell receptors. Once inside the cell, the virus relies on several enzymes and proteins to replicate and produce new viral particles. Among these, the main protease (Mpro) and papain-like protease (PLpro) are two essential viral enzymes responsible for processing viral polyproteins into functional proteins required for viral replication. Mpro is involved in cleaving viral protein chains into smaller active units, whereas PLpro not only supports viral replication but also suppresses the host immune response, helping the virus evade immune detection. Because humans do not possess closely related enzymes, these proteases are considered attractive and selective targets for antiviral drug development. [11–15]

Various therapeutic strategies have been explored to combat COVID-19, including vaccines, antiviral drugs, and immunomodulatory agents. Several approved antiviral drugs act by targeting different stages of the viral life cycle, such as viral entry, RNA synthesis, and protein processing. However, the continuous emergence of SARS-CoV-2 variants, particularly highly transmissible strains such as Omicron, has raised concerns regarding treatment effectiveness and viral resistance. These challenges highlight the need for the discovery and development of new antiviral compounds with improved efficacy. [16–23]Among the potential therapeutic targets, papain-like protease (PLpro) has gained considerable attention because of its dual role in viral replication and immune evasion. Inhibiting PLpro can simultaneously block virus multiplication and restore the host immune response, making it a promising target for anti-COVID drug discovery. Therefore, computational approaches such as molecular docking and in-silico screening have become valuable tools for identifying and evaluating potential PLpro inhibitors. These methods provide a rapid and cost-effective strategy for the discovery of novel therapeutic candidates against SARS-CoV-2. [13,14,22–25]

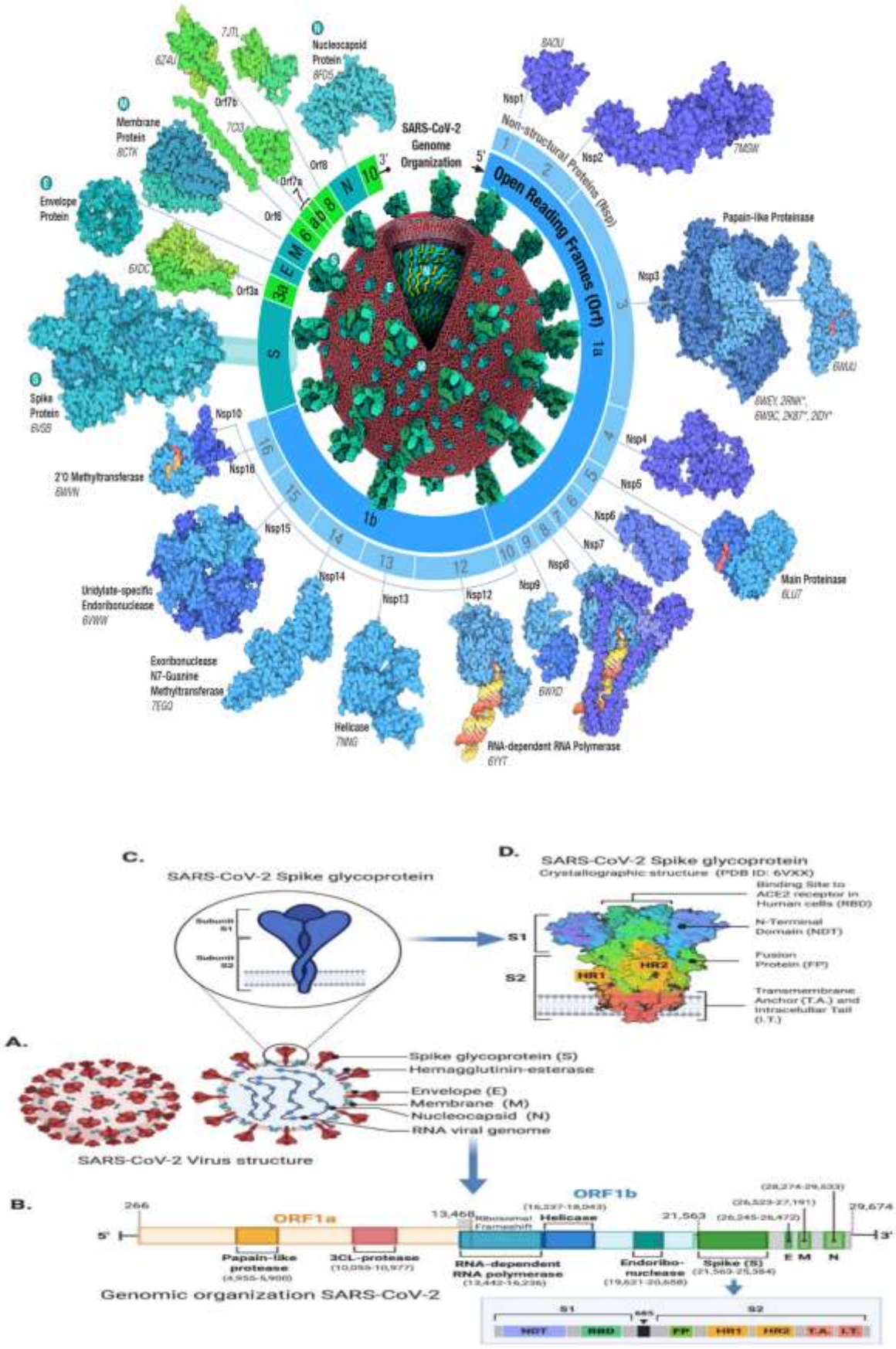

Fig.No.1 SARS-CoV-2: Structure,Genome and Proteins

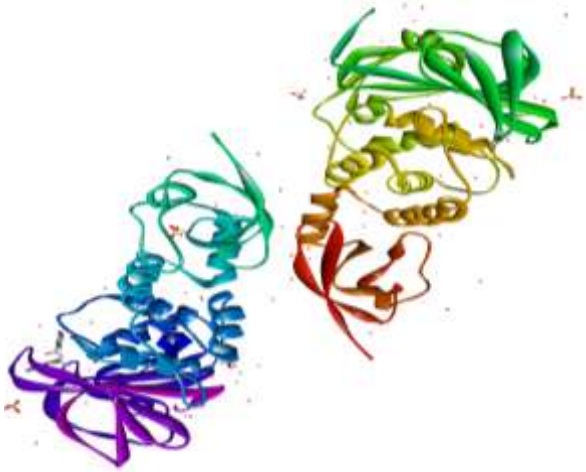

Fig.No.2 Crystal Structure of wild type SARS-CoV-2 Papain-like protease(PLPro) [PDB ID:7JRN]

GRL-0617 is widely recognized as a non-covalent inhibitor of the SARS-CoV-2 papain-like protease (PLpro) and has been extensively used as a reference compound in PLpro-related studies. It has been shown to bind near the active site of PLpro, where access of viral substrates is restricted and the processing of viral polyproteins is reduced. In addition, the immune-evasion function of PLpro is reported to be suppressed when GRL-0617 is present, which may support the host antiviral response. Owing to its well-defined binding mode and consistent inhibitory behavior, GRL-0617 is commonly included in in-silico, structural, and biochemical evaluations as a standard compound for comparison during the assessment of potential PLpro inhibitors.

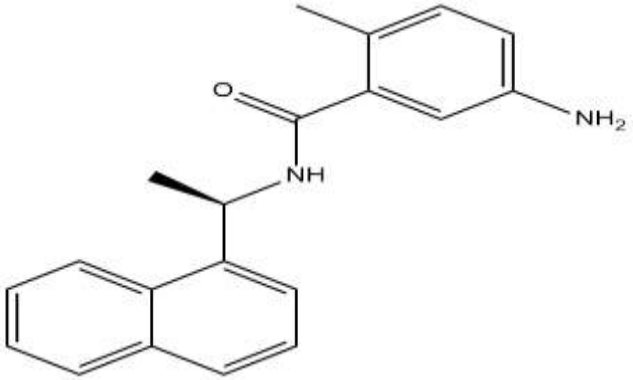

Fig No.3 GRL-0617

VIR-250 has been developed as a covalent inhibitor that targets the catalytic cysteine residue of PLpro. Through covalent bond formation, the enzymatic activity of PLpro is effectively suppressed. Structural studies have indicated that VIR-250 fits well within the PLpro active site and forms stable interactions that contribute to strong inhibition. Owing to its potent and irreversible binding mechanism, VIR-250 is frequently included in comparative in-silico evaluations.

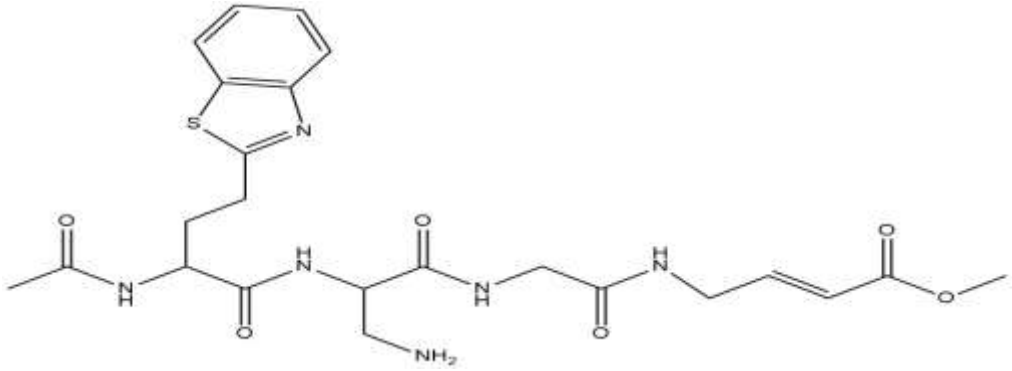

Fig No.4 VIR-250

VIR-251 is structurally related to VIR-250 and has been designed with modifications aimed at improving binding efficiency and specificity. Similar to VIR-250, PLpro inhibition is achieved through covalent interaction with the catalytic cysteine residue. Additional stabilizing interactions within the binding pocket have been suggested, which may enhance inhibitory performance. As a result, VIR-251 is often evaluated alongside other PLpro inhibitors to compare binding affinity and interaction patterns.

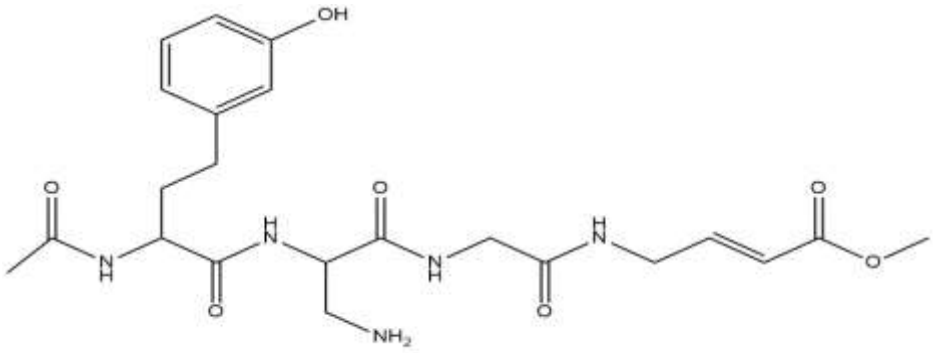

Fig No.5 VIR-251

Methodology

Materials used for the in silico study

The softwares will be used to execute this project in silico work is UCSF-Chimera© (version 1.18) software for optimizing ligands and for molecular docking since it abhors AutoDock Vina module; UCSF-Chimera© (version 1.13) software will be used for protein target preparation for docking. Discovery studio (Biovia) 4.5 molecular Graphic system version 2.4.1 will be used for preparing protein-ligand complexes after docking and for 3D and 2D visualization of protein- ligand complexes. All softwares will be run on a personal computer,Dell brand with a processor of 13th generation Intel Core i5, 1.30 GHz, 16 GB RAM, and 128 GB hard disk.

Protein targets selection and preparation

Crystal structure of the wild type SARS-CoV-2 papain-like protease(PLPro) is selected for this study. The 3D crystal structures of the receptors were retrieved from the Protein Data Bank (PDB) (www.pdb.org/pdb) with PDB IDs of 7JRN (https://www.rcsb.org/structure/7JRN) for PLpro is used. Chain A of protein receptors is selected and cleaned from heteroatoms,using the Dock preparation tool of UCSF-Chimera© (version 1.18) software.

Ligand preparation

Chemical structure of the ligands are drawn and imported followed by geometry optimization and assigning charges. Kollmann charges are added.Non-polar charges are merged. Net charge on the ligand are neutralised to zero and active site identification and grid generation on the protein for ligand binding are defined.

Docking Simulation

The docking process is conducted using specialized software UCSF chimera to predict the optimal binding pose and estimate binding affinity through scoring functions. Finally, post-docking analysis is conducted, which includes evaluating binding energy, hydrogen bonds, and other interactions to interpret the biological relevance and guide further experimental or computational studies. The lowest binding energy (BE, kcal/mol) and root mean square deviation (RMSD) conformation are considered as the most suitable docking pose. Throughout this in silico investigation, an exhaustiveness of 8 is used for docking, and the number of modes are set to 9 so as to achieve more accurate and reliable results. The interaction between ligands and proteins are prepared, visualized, and analyzed by Discovery Studio 2016 respectively.

This work includes analysis for the RMSD as a function of time of the 7JRN.During simulations, RMSD is used as a critical parameter to gauge the conformational changes of ligands within the active site of the protein ligand complex, which shows initial oscillations. In contrast, a lower RMSD value in the ligand with the 7JRN protein structure implies enhanced stability and satisfaction within the binding site.

The physicochemical, In-silico ADME, and drug-likeness parameters of the identified potentially active candidate compounds are computed using the Swiss ADME online program which is developed by the Swiss Institute of Bioinformatics and freely available at www.swissadme.ch (Daina et al., 2017. SwissADME gives free access to several parameters and predictive models in order to compute the physicochemistry and estimate the pharmacokinetics, drug-likeness and medicinal chemistry friendliness of one or several small molecules

The compounds with high-ranking binding energy scores are subjected to this part of the screening process. Simple physicochemical properties such as molecular weight (MW), molecular refractivity (MR), atom counts, and polar surface area (PSA) are computed. This is implemented by the OpenBabel, version 2.3.0 (O'Boyle et al., 2011). Drug-likeness candidature is implemented by Lipinski (2001), Ghose (1999), Veber (2002), Egan (2000), and Muegge (2001) rules of 5 (RO5) screening. The Abbot Bioavailability scores are computed to predict the probability of a compound to have at least 10% oral bioavailability by relying on total charge, TPSA, and violation of the Lipinski's filter. Lipophilicity are implemented with iLOGP, XLOGP3, WLOGP, MLOGP, and SILICOS-IT models from which a consensus log Po/w are determined (Daina et al., 2017). The solubility (log S) of the selected ligands is implemented by three different models: ESOL (Delaney, 2004), Ali (Ali et al., 2012), and SILICOS-IT (Daina et al., 2017).

ADME Report

1.GRL-0617

Table.II. ADME of GRL-0617

Molecule 1

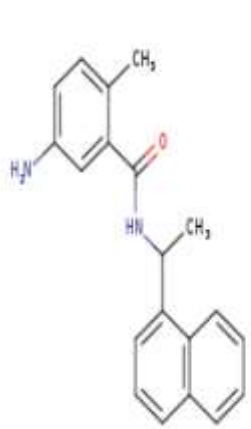

SMILES Nc1ccc(c(c1)C(=O)NC(c1cccc2c1cccc2)C)C

Physicochemical Properties	
Formula	C20H20N2O
Molecular weight	304.39 g/mol
Num. heavy atoms	23
Num. arom. heavy atoms	16
Fraction Csp3	0.15
Num. rotatable bonds	4
Num. H-bond acceptors	1
Num. H-bond donors	2
Molar Refractivity	96.61
TPSA	55.12 Å²

Lipophilicity	
Log $P_{o/w}$ (iLOGP)	2.69
Log $P_{o/w}$ (XLOGP3)	4.03
Log $P_{o/w}$ (WLOGP)	3.91
Log $P_{o/w}$ (MLOGP)	3.65
Log $P_{o/w}$ (SILICOS-IT)	4.02
Consensus Log $P_{o/w}$	3.66

Water Solubility	
Log S (ESOL)	-4.52
Solubility	9.26e-03 mg/ml ; 3.04e-05 mol/l
Class	Moderately soluble
Log S (Ali)	-4.89
Solubility	3.92e-03 mg/ml ; 1.29e-05 mol/l
Class	Moderately soluble
Log S (SILICOS-IT)	-7.04
Solubility	2.77e-05 mg/ml ; 9.10e-08 mol/l
Class	Poorly soluble

Pharmacokinetics	
GI absorption	High
BBB permeant	Yes
P-gp substrate	Yes
CYP1A2 inhibitor	No
CYP2C19 inhibitor	Yes
CYP2C9 inhibitor	Yes
CYP2D6 inhibitor	Yes
CYP3A4 inhibitor	Yes
Log K_p (skin permeation)	-5.30 cm/s

Druglikeness	
Lipinski	Yes; 0 violation
Ghose	Yes
Veber	Yes
Egan	Yes
Muegge	Yes
Bioavailability Score	0.55

Medicinal Chemistry	
PAINS	0 alert
Brenk	1 alert: aniline
Leadlikeness	No; 1 violation: XLOGP3>3.5
Synthetic accessibility	2.26

2.VIR-250

Table.III. ADME of VIR-250

Molecule 2

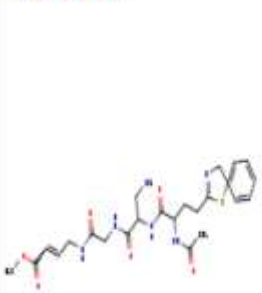

SMILES NCC(C(=O)NCC(=O)NC/C=C/C(=O)OC)NC(=O)C(NC(=O)C)CCC1=NC(C)2(=CC=CC=C2)S1

Physicochemical Properties	
Formula	C24H33N6O6S
Molecular weight	533.62 g/mol
Num. heavy atoms	37
Num. arom. heavy atoms	0
Fraction Csp3	0.42
Num. rotatable bonds	18
Num. H-bond acceptors	8
Num. H-bond donors	5
Molar Refractivity	143.02
TPSA	206.38 Å²

Lipophilicity	
Log $P_{o/w}$ (iLOGP)	0.00
Log $P_{o/w}$ (XLOGP3)	-1.31
Log $P_{o/w}$ (WLOGP)	-1.42
Log $P_{o/w}$ (MLOGP)	-1.56
Log $P_{o/w}$ (SILICOS-IT)	1.28
Consensus Log $P_{o/w}$	-0.60

Water Solubility	
Log S (ESOL)	-1.14
Solubility	3.91e+01 mg/ml ; 7.33e-02 mol/l
Class	Very soluble
Log S (Ali)	-2.53
Solubility	1.59e+00 mg/ml ; 2.98e-03 mol/l
Class	Soluble
Log S (SILICOS-IT)	-3.16
Solubility	3.68e-01 mg/ml ; 6.90e-04 mol/l
Class	Soluble

Pharmacokinetics	
GI absorption	Low
BBB permeant	No
P-gp substrate	No
CYP1A2 inhibitor	No
CYP2C19 inhibitor	No
CYP2C9 inhibitor	No
CYP2D6 inhibitor	No
CYP3A4 inhibitor	No
Log K_p (skin permeation)	-10.49 cm/s

Druglikeness	
Lipinski	No; 2 violations: MW>500, NorO>10
Ghose	No; 3 violations: MW>480, WLOGP<-0.4, MR>130
Veber	No; 2 violations: Rotors>10, TPSA>140
Egan	No; 1 violation: TPSA>131.6
Muegge	No; 2 violations: TPSA>150, Rotors>15
Bioavailability Score	0.17

Medicinal Chemistry	
PAINS	0 alert
Brenk	1 alert: michael_acceptor_1
Leadlikeness	No; 2 violations: MW>350, Rotors>7
Synthetic accessibility	6.14

3.VIR-251

Table.IV. ADME of VIR-251

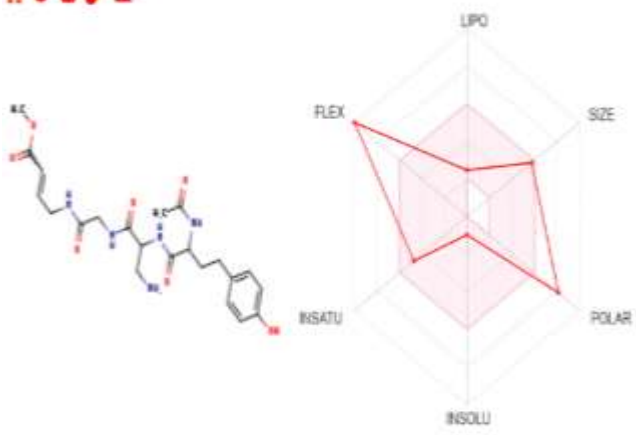

SMILES NCC(C(=O)NCC(=O)NC/C=C/C(=O)OC)NC(=O)C(NC(=O)C)CCc1ccc(cc1)O

Physicochemical Properties	
Formula	C22H31N5O7
Molecular weight	477.51 g/mol
Num. heavy atoms	34
Num. arom. heavy atoms	6
Fraction Csp3	0.41
Num. rotatable bonds	18
Num. H-bond acceptors	8
Num. H-bond donors	6
Molar Refractivity	121.06
TPSA	188.95 Å²

Lipophilicity	
Log $P_{o/w}$ (iLOGP)	1.78
Log $P_{o/w}$ (XLOGP3)	-1.19
Log $P_{o/w}$ (WLOGP)	-1.77
Log $P_{o/w}$ (MLOGP)	-1.25
Log $P_{o/w}$ (SILICOS-IT)	0.71
Consensus Log $P_{o/w}$	-0.34

Water Solubility	
Log S (ESOL)	-0.99
Solubility	4.85e+01 mg/ml ; 1.02e-01 mol/l
Class	Very soluble
Log S (Ali)	-2.28
Solubility	2.48e+00 mg/ml ; 5.20e-03 mol/l
Class	Soluble
Log S (SILICOS-IT)	-3.99
Solubility	4.92e-02 mg/ml ; 1.03e-04 mol/l
Class	Soluble

Pharmacokinetics	
GI absorption	Low
BBB permeant	No
P-gp substrate	Yes
CYP1A2 inhibitor	No
CYP2C19 inhibitor	No
CYP2C9 inhibitor	No
CYP2D6 inhibitor	No
CYP3A4 inhibitor	No
Log K_p (skin permeation)	-10.06 cm/s

Druglikeness	
Lipinski	No; 2 violations: NorO>10, NHorOH>5
Ghose	No; 1 violation: WLOGP<-0.4
Veber	No; 2 violations: Rotors>10, TPSA>140
Egan	No; 1 violation: TPSA>131.6
Muegge	No; 3 violations: TPSA>150, Rotors>15, H-don>5
Bioavailability Score	0.17

Medicinal Chemistry	
PAINS	0 alert
Brenk	1 alert: michael_acceptor_1
Leadlikeness	No; 2 violations: MW>350, Rotors>7
Synthetic accessibility	4.04

Physicochemical Properties of ligands using Swiss ADME

Table.V.Physicochemical Properties of ligands using Swiss ADME

Properties	**GRL-0617**	**VIR-250**	**VIR-251**
Formula	$C_{20}H_{20}N_2O$	$C_{24}H_{33}N_6O_6S$	$C_{22}H_{31}N_5O_7$
Molecular Weight	304.39 g/mol	533.62 g/mol	477.51 g/mol
No. of heavy atoms	23	37	34
No. of rotatable bond	4	18	18
No. of H-Bond Donors	2	5	6
Molecular Refractivity	95.61	143.02	121.06
Topological Polar Surface Area	55.12 A^2	206.38 A^2	188.95 A^2

Physicochemical properties of ligands using Swiss ADME Lipophilicity and Water Solubility

Table.VI. Physicochemical properties of ligands using Swiss ADME Lipophilicity and Water Solubility

Properties	**Lipophilicity**	**Water Solubility**		
	Consensus Log $P_{o/w}$	**Log S[Ali]**	**Log S [SILICOS-IT]**	**Class**
GRL-0617	3.66	-4.89	-7.04	Poorly Soluble
VIR-250	-0.60	-2.53	-3.16	Soluble
VIR-251	-0.34	-2.28	-3.99	Soluble

Pharmacokinetic predictions of ligands using Swiss ADME

Table.VII. Pharmacokinetic predictions of ligands using Swiss ADME

Parameters	GRL-0617	VIR-250	VIR-251
GI Absorption	High	Low	Low
BBB Permeant	Yes	No	No
P-gp Substrate	Yes	No	Yes
CYP1A2 inhibitor	No	No	No
CYP2C19 inhibitor	Yes	No	No
CYP2C9 inhibitor	Yes	No	No
CYP2D6 inhibitor	Yes	No	No
CYP3A4 inhibitor	Yes	No	No

Drug Likeness Predictions using Swiss ADME

Table.VIII. Drug Likeness Predictions using Swiss ADME

Properties	GRL-0617	VIR-250	VIR-251
Lipinski	Yes	No	No
Ghose	Yes	No	No
Veber	Yes	No	No
Egan	Yes	No	No
Muegge	Yes	No	No
Bioavailability Score	0.55	0.17	0.17
Leadlikeness	No	No	No

SMILES Code using Swiss ADME

Table.IX. SMILES Code using Swiss ADME

Inhibitors	SMILES Code
GRL-0617	Nc1ccc(c(c1)C(=O)NC(c1cccc2c1cccc2)C)C
VIR-250	NCC(C(=O)NCC(=O)NC/C=C/C(=O)OC)NC(=O)C(NC(=O)C)CCC1=NC[C]2(=CC=CC=C2)S1
VIR-251	NCC(C(=O)NCC(=O)NC/C=C/C(=O)OC)NC(=O)C(NC(=O)C)CCc1ccc(cc1)O

Experimental work

GRL-0617

IUPAC:[5-amino-2-methyl-N-[(1R)-1-(napthalen-1-yl)ethyl]benzamide]

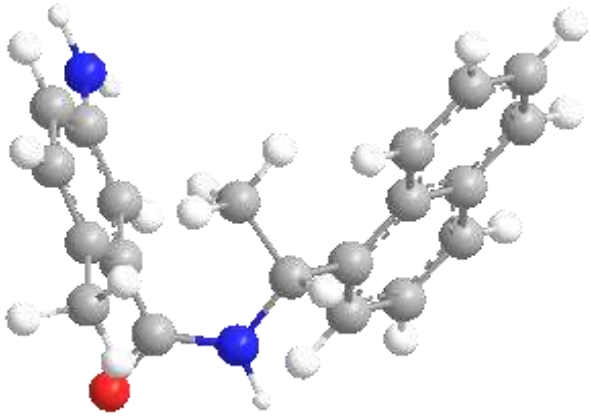

Fig No.6 GRL-0617 3D

Table.X. Dockscore of GRL-0617

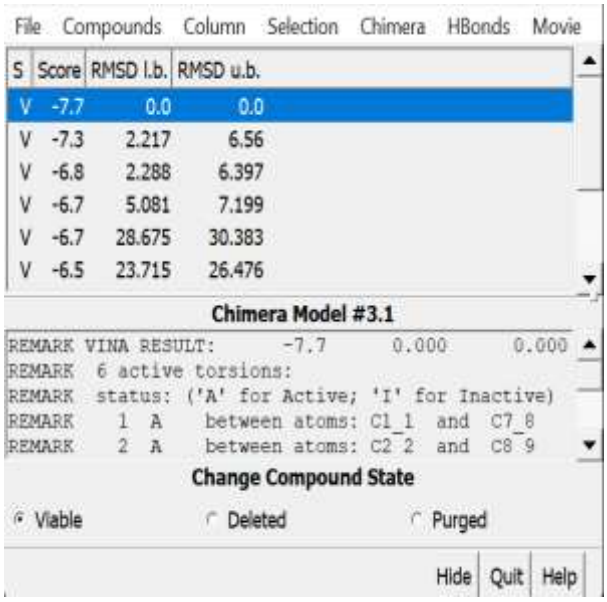

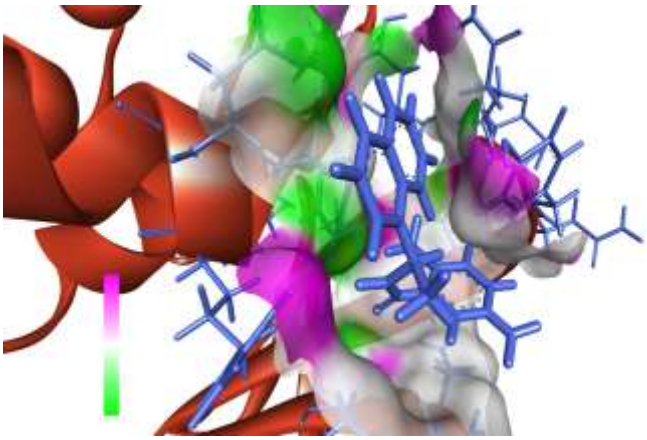

Fig No.7 Dock of GRL-0617

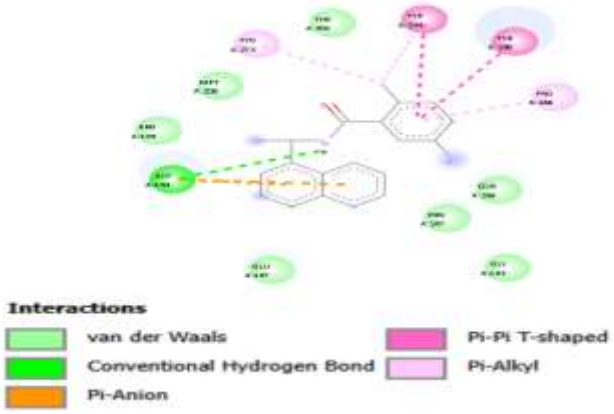

Fig No.8 GRL-0617 2D Interaction

VIR-250

IUPAC: Methyl(E)-7-(aminomethyl)-4-[2-(1,3-benzothiazol-2-yl)ethyl]-2,5,8,11-tetraoxo-3,6,9,12-tetraazahexadec-14-en-16-oate

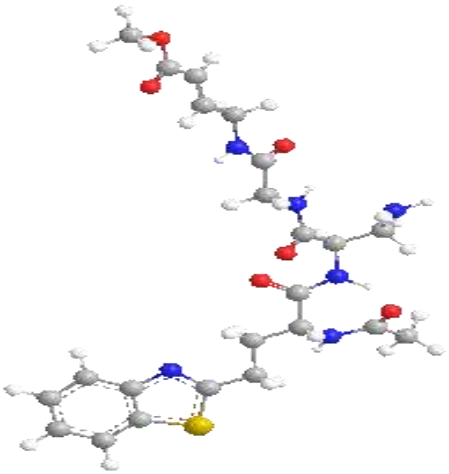

Fig No.9 VIR-250 3D

Table.XI. Dockscore of VIR-250

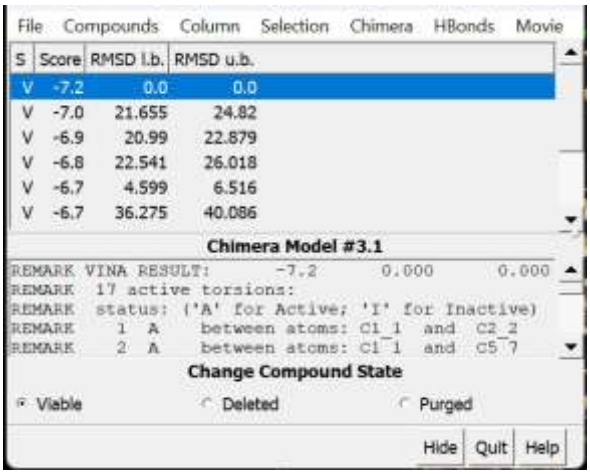

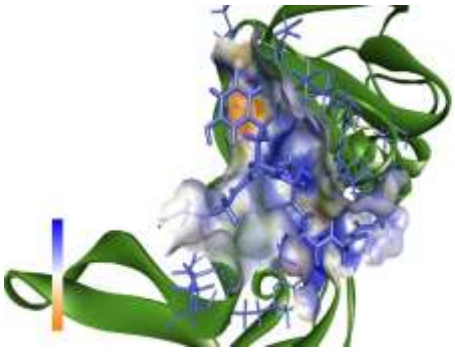

Fig No.10 Dock of VIR-250

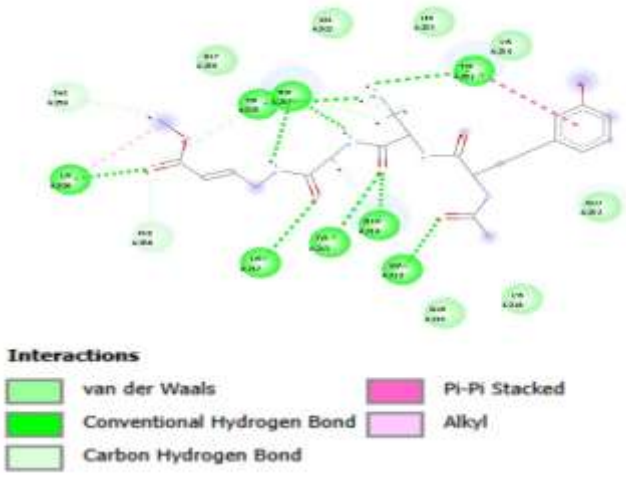

Fig No.11 VIR-250 2D Interaction

VIR-251

IUPAC:Methyl(E)-10-(aminomethyl)-13-[2-(3-hydroxyphenyl)ethyl]-6,9,12,15-tetraoxo-5,8,11,14-tetraazahexadec-2-en-1-oate

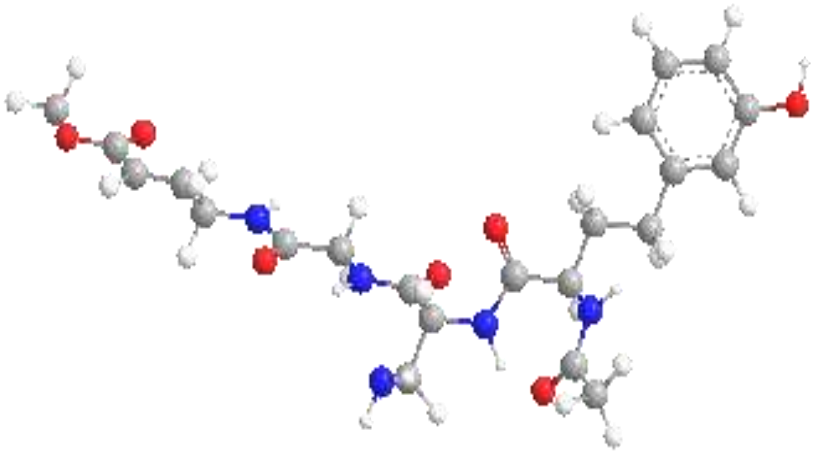

Fig No.12 VIR-251 3D

Table.XII. Dockscore of VIR-251

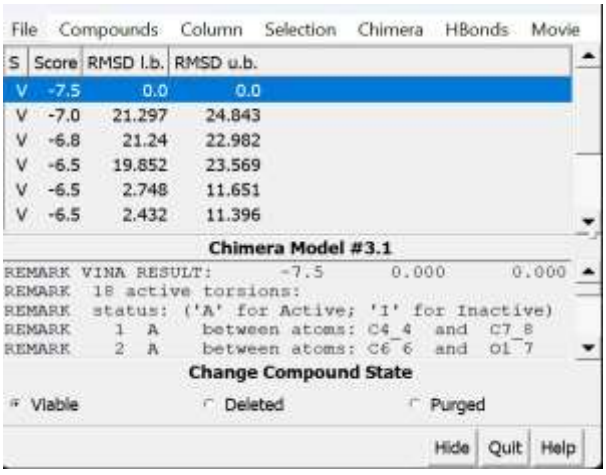

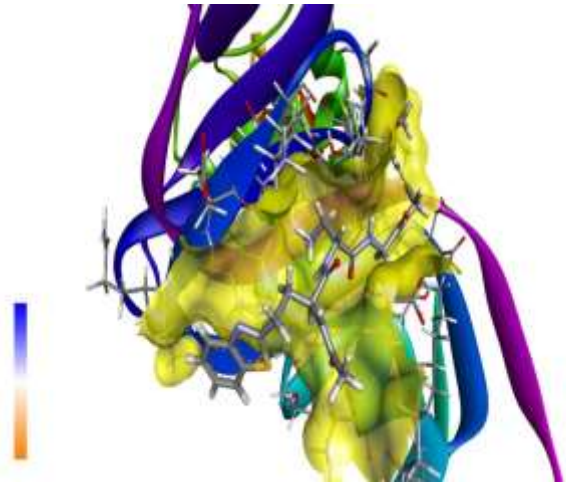

Fig No.13 Dock of VIR-251

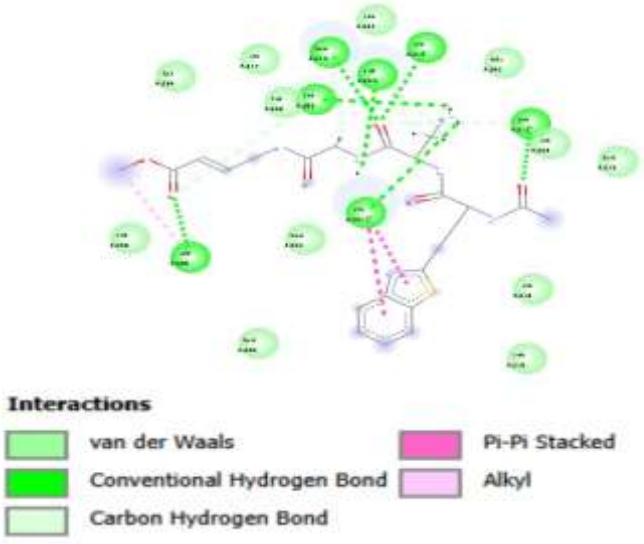

Fig No.14 VIR-251 2D Interaction

Results

GRL-0167 Interaction Types and Interactiom Residues

Table.XIII. GRL-0167 Interaction Types and Interactiom Residues

Interaction Types	Interaction Residues
van der Waals	ARG A:166 GLU A:167 MET A:206 THR A:301 GLN A:269 PRO A:247 GLY A:163
Conventional H-Bond	ASP A:164
Pi-Anion	ASP A:164
Pi-Alkyl	TYR A:273

	PRO A:248
Pi-Pi T-shaped	TYR A:264 TYR A:268

VIR-250 Interaction Types and Interactiom Residues

Table.XIV. VIR-250 Interaction Types and Interactiom Residues

Interaction Types	Interaction Residues
van der Waals	GLY A:256 VAL A:303 LEU A:253 LYS A:254 GLU A:252 LYS A:218 GLN A:215
Conventional H-Bond	LYS A:306 TYR A:306 THR A:257 LYS A:217 TYR A:213 TYR A:251 GLU A:214 SER A:212
Carbon Hydrogen Bond	PHE A:258 THR A:259
Pi-Pi Stacked	TYR A:251
Alkyl	LYS A:306

VIR-251 Interaction Types and Interactiom Residues

Table.XV. VIR-251 Interaction Types and Interactiom Residues

Interaction Types	Interaction Residues
van der Waals	GLL A:127 ASN A:124 ALA A:124 ASP A:157 AS7 A:157 GLY A:158 ASP A:166 IAS A:124 VIES A:124 HIS A:126 GLV A:126 GLY A:145
Conventional H-Bond	PHE A:157

	HIS A:129 PHE A:129 THP A:124 PHE A:241 GLY A:158 VIES A:124
Pi-Pi Stacked	HIS A:129
Alkyl	PHE A:157

Discussion

In the present work, a comparative in-silico study is carried out to examine selected reverse papain-like protease (PLpro) inhibitors against SARS-CoV-2. The study is designed to explore the interaction of these inhibitors with PLpro using computational tools, with the aim of developing a preliminary understanding of their binding behavior.PLpro is selected as the target enzyme due to its established role in viral replication and host immune evasion.Molecular docking studies are performed to observe the binding orientation of each inhibitor within the PLpro active site. Through this approach, potential interactions between the enzyme and inhibitors are identified, including hydrogen bonding and hydrophobic contacts. These observations are recorded to provide structural insight into enzyme–inhibitor interactions.In addition to docking analysis, in-silico evaluation of drug-likeness and ADMET properties are conducted to obtain preliminary information on the pharmacokinetic feasibility of the selected compounds. The data generated from these analyses are presented as supportive findings.Overall, a systematic computational framework is established for the comparative evaluation of reverse PLpro inhibitors against SARS-CoV.

Reference

1. *World Health Organization. Coronavirus disease (COVID-19): Situation Reports and Global Research. WHO, Geneva.*
2. *World Health Organization. COVID-19 Strategic Preparedness and Response Plan. WHO, 2020–2023.*
3. Huang, C., et al. (2020). *Clinical features of patients infected with 2019 novel coronavirus in Wuhan, China*. **The Lancet**, 395(10223), 497–506.
4. Wu, Z., & McGoogan, J. M. (2020). *Characteristics of and important lessons from the COVID-19 outbreak in China*. **JAMA**, 323(13), 1239–1242.
5. World Health Organization. (2020). *An R&D Blueprint for action to prevent epidemics*. WHO.
6. Bergeri, I., et al. (2022). *Global SARS-CoV-2 seroepidemiology from WHO Unity Studies*. **The Lancet**, 399(10334), 1516–1526.
7. World Health Organization. (2021). *Emergency Use Listing procedure for COVID-19 vaccines*. WHO.
8. Polack, F. P., et al. (2020). *Safety and efficacy of the BNT162b2 mRNA COVID-19 vaccine*. **New England Journal of Medicine**, 383, 2603–2615.
9. Andersen, K. G., et al. (2020). *The proximal origin of SARS-CoV-2*. **Nature Medicine**, 26, 450–452.
10. World Health Organization. (2021). *WHO-convened global study of origins of SARS-CoV-2*.

11. Zhang, L., et al. (2020). *Crystal structure of SARS-CoV-2 main protease provides a basis for drug design*. **Science**, 368(6489), 409–412.
12. Ullrich, S., & Nitsche, C. (2020). *The SARS-CoV-2 main protease as drug target*. **Bioorganic & Medicinal Chemistry Letters**, 30(17), 127377.
13. Shin, D., et al. (2020). *Papain-like protease regulates SARS-CoV-2 viral spread and innate immunity*. **Nature**, 587, 657–662.
14. Klemm, T., et al. (2020). *Mechanism and inhibition of the papain-like protease of SARS-CoV-2*. **EMBO Journal**, 39(18), e106275.
15. *Rang, H. P., Dale, M. M., Ritter, J. M., & Flower, R. J. (2016). Rang and Dale's Pharmacology (8th ed.). Elsevier.*
16. Hoffmann, M., et al. (2020). *SARS-CoV-2 cell entry depends on ACE2 and TMPRSS2*. **Cell**, 181(2), 271–280.
17. Walls, A. C., et al. (2020). *Structure, function, and antigenicity of the SARS-CoV-2 spike glycoprotein*. **Cell**, 181(2), 281–292.
18. Gordon, C. J., et al. (2020). *Remdesivir is a direct-acting antiviral that inhibits SARS-CoV-2 RdRp*. **Journal of Biological Chemistry**, 295(20), 6785–6797.
19. Gao, Y., et al. (2020). *Structure of the RNA-dependent RNA polymerase from COVID-19 virus*. **Science**, 368(6492), 779–782.
20. Mehta, P., et al. (2020). *COVID-19: consider cytokine storm syndromes and immunosuppression*. **The Lancet**, 395(10229), 1033–1034.
21. Tay, M. Z., et al. (2020). *The trinity of COVID-19: immunity, inflammation and intervention*. **Nature Reviews Immunology**, 20, 363–374.
22. Ratia, K., et al. (2008). *A non-covalent class of papain-like protease inhibitors blocks SARS virus replication*. **Proceedings of the National Academy of Sciences (PNAS)**, 105(42), 16119–16124.
23. Freitas, B. T., et al. (2020). *Characterization and non-covalent inhibition of SARS-CoV-2 PLpro*. **ACS Infectious Diseases**, 6(8), 2099–2109.
24. Rut, W., et al. (2020). *Activity profiling and crystal structures of inhibitor-bound SARS-CoV-2 papain-like protease*. **Nature Communications**, 11, 4431.
25. Osipiuk, J., et al. (2021). *Structure-based drug design of PLpro inhibitors*. **Nature Communications**, 12, 4659.